Heterojunction perovskite microrods prepared by remote-controlled vacancy filling and halide exchange

Md Shahjahan,[1] Ken-ichi Yuyama,[1,2,*] Takuya Okamoto,[2] Vasudevanpillai Biju[1,2,*]
[1]Graduate School of Environmental Science, and [2]Research Institute for Electronic Science, Hokkaido University, Sapporo, Hokkaido 001-0020, Japan
*Corresponding author yuyama@es.hokudai.ac.jp; biju@es.hokudai.ac.jp

Abstract. Anion exchange reaction tunes the bandgap of halide perovskites, which proceeds by the migration of the ions through the halide vacancies. We report the preparation of the heterojunction perovskite microrods by optically controlled localized halide vacancy filling, and halide exchange leading to colour tuning in the $MAPbBr_3$ microrod crystals. The exchange reaction is homogeneously suppressed by treating the crystal with a halide precursor solution, whereas the reaction is locally inhibited at the specific site of a crystal by filling the halide vacancies using a tightly focused beam of a near-infrared laser. By controlling the density of halide vacancies at the specific site of the crystal, we control the rate of non-radiative recombination of charge carriers in the crystal. This halide vacancy filling by the remote-controlled reaction helps us to locally control the crystal quality and photoluminescence for designing perovskite-based high quality photovoltaic and optoelectronic devices.

TOC Graphic

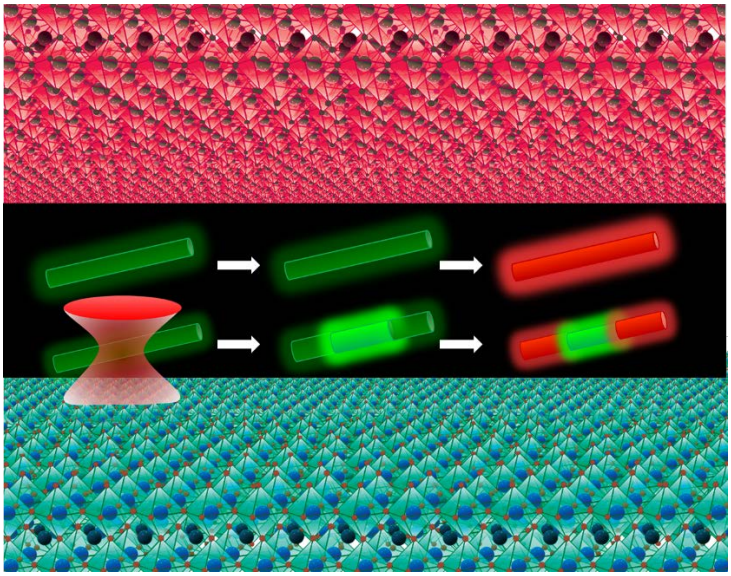

Keywords: Halide perovskites; photoluminescence; halide exchange; laser trapping; vacancy filling

Halide perovskites have given researchers an indisputable curiosity toward the development of cost-effective, and solution-processable next-generation photovoltaic and optoelectronic devices.[1] In general, the solution-processed halide perovskites are of low-quality due to an abundance of crystal defects. Nevertheless, when compared with a conventional semiconductor, perovskite crystals show superior properties such as long-range anion diffusion, wide optical absorption range, excellent photoluminescence (PL) quantum efficiencies, low exciton binding energy, and high electron and hole mobilities.[2] In addition, the crystal lattices of perovskites undergo rapid exchange reactions when exposed to reactive halide precursors, which results in the bandgap tuning throughout the broad spectral range from visible to near-infrared (NIR).[3]

The quality of perovskite crystals is strongly affected by the nature and density of defects, particularly anion or cation vacancies.[4] These defects generate structural distortions and induce anion and charge migrations or segregations, lowering the performance of perovskite devices. Therefore, it is essential to figure out the nature and density of the defects and reduce or remove them to improve the quality of such devices. Defects of perovskite nanocrystals, bulk crystals, and thin films are studied theoretically and experimentally. For example, the free-energy change of defect formation can be computed from a molecular simulation. The chemical compositions of perovskite crystals can be verified with techniques such as energy dispersive X-ray (EDX) or (X-ray photoelectron spectroscopy(XPS).[5] However, quantification of the defect density in a perovskite crystal is still challenging. Time-resolved PL spectroscopy reveals the relaxation processes of photogenerated charge carriers, which also helps to estimate the trap state density. While these sophisticated methods provide direct information of defects, we found the halide vacancies have a critical role in localized anion exchange reaction.

Here, we report that the halide exchange reaction of perovskite microrod crystals can be suppressed by pre-treating the crystal with the constituent halide ions. A green emissive as-grown $MAPbBr_3$ ($MA = CH_3NH_3^+$) crystal shows the rapid Br^--to-I^- exchange reaction in an MAI solution and the PL emission changes to red due to the formation of $MAPb(Br{\cdot}I)_3$. Conversely, a $MAPbBr_3$ microrod pre-treated with MABr remained green emissive even after prolonged incubation with a MAI solution. We consider that the bromide vacancy filling suppresses the exchange. In addition, such vacancy filling is induced in a spatially resolved manner by irradiating with a tightly focused non-resonant laser beam, and subsequently, the exchange reaction proceeds only in the non-irradiated part. These findings provide us with a new way to optimize the optoelectronic properties of perovskite crystals at the desired location.

The scheme in Figure 1a shows the experimental process for halide vacancy filling of a $MAPbBr_3$ microrod. $MAPbBr_3$ microcrystals with the rod shape were prepared in the following process. The precursor solution of $MAPbBr_3$ (1.3 M) was prepared by dissolving

equimolar amounts of MABr and $PbBr_2$ in *N,N*-dimethylformamide (DMF). Based on the reported solubility curve, the saturation degree was calculated at 0.85 for this solution at room temperature.[6] To decrease the precursors' solubility, the prepared solution was mixed with γ-butyrolactone (1:1, v:v), through which a supersaturated solution was obtained. A small amount (ca. 0.5 µL) of this solution was placed in a sample silicone chamber, which was fabricated by gluing an O-ring shaped silicon rubber on a cover glass with silicone glue. Spontaneous crystallization of $MAPbBr_3$ occurred within 2–3 min. After removing the remaining solution with a filter paper, the solution of MAI (375 µM), prepared in a mixture of 1-hexadecene and isopropanol (100:1, v/v) was added to the chamber to induce the bromide-to- iodide exchange reaction [Figure 1a (i and iii)].

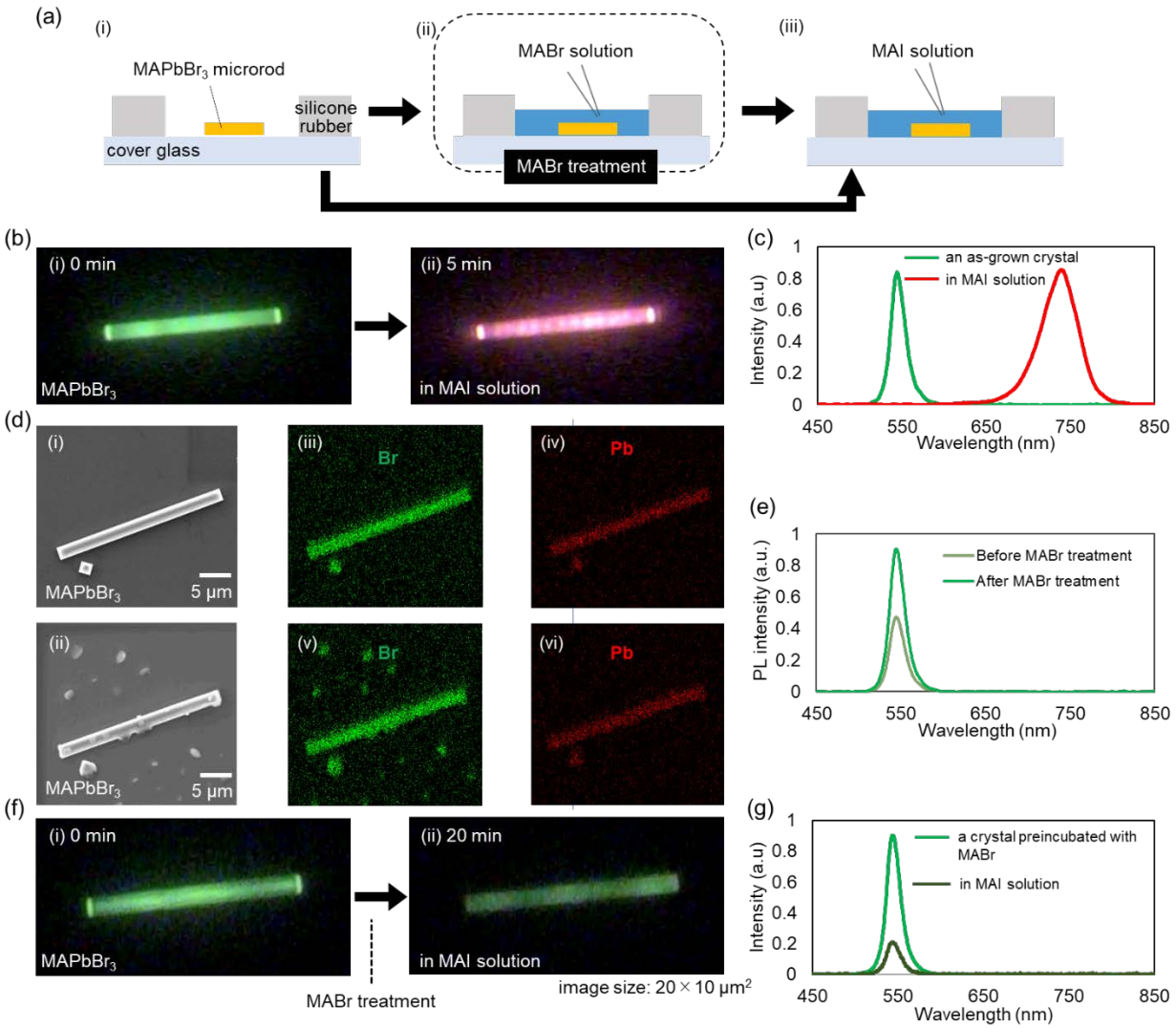

Figure 1. (a) A scheme of the experimental procedure for halide filling and exchange reactions. (b, f) PL images and (c, e, g) PL spectra of an as-grown $MAPbBr_3$ microrod crystal and the crystal in (e) a MABr or (c, g) a MAI solution. The crystal [f(i)] was treated with a MABr solution prior to an incubation with the MAI solution. (d) (i, ii) SEM images and (iii-vi) EDX elemental maps of a $MAPbBr_3$ microrod crystal (i, iii, iv) before and (ii, v, vi) after immersing in a MABr solution.

First, we recorded the PL images of an as-grown $MAPbBr_3$ microrod crystal and the crystal in the reaction solution of MAI (Figure 1b). These images were obtained upon exciting the crystal with a 405-nm excitation laser beam (Supplementary Information (SI). Before the addition of the MAI solution, the $MAPbBr_3$ crystal showed intense green emission in the whole area [Figure 1b (i)]. In the MAI solution, the green emissive as-grown crystal gradually changed its emission colour into red. At about 5-min, the whole crystal showed the red PL [Figure 1b (ii)]. This change from the green to the red PL is induced by the resultant $MAPb(Br{\cdot}I)_3$, which is through the halide exchange reaction between bromide ions in the crystal and iodide ions in the solution. Figure 1c shows the PL spectra of the crystal before and after the addition of the MAI solution. These spectra were measured at the center part of the crystal. Initially, the PL spectral maximum was at 545 nm. This maximum is well-matched with the reported value for a $MAPbBr_3$ bulk crystal.[7] Conversely, the PL spectral maximum was redshifted to 740 nm after 5-min incubation with the MAI solution. The broad spectrum PL spectrum of the halide exchanged crystal is attributed to the formation of $MAPb(BrI)_3$ with different Br and I compositions. However, the PL spectral maximum indicates that the exchange reaction resulted in the formation of predominantly $MAPbBr_{0.8}I_{2.2}$, which is based on the reported relation between PL spectral maxima and the halide composition.[3c]

To evaluate the role of the halide vacancies on the exchange reaction, we pre-treated the as-grown $MAPbBr_3$ microrod with a MABr solution [Figure 1a (ii and iii)]. Here, the synthesized crystal was immersed in the 1-hexadecene/isopropanol (100:1) solution of MABr (375 μM) for 5-min, after which the MABr solution was removed. We examined the Br vacancy filling in as-grown $MAPbBr_3$ microrods by recording the SEM-EDX (Figure 1d) and PL (Figure 1e) spectra of the rods before and after immersing in a MABr solution (375 μM). Figure 1d shows the SEM images (i and ii) and EDX elemental maps (iii-vi) of a microrod before and after the Br vacancy filling. The Br composition of the microrod was increased by 9% after immersing in the solution, confirming vacancy filling. Similarly to an increase in the bromide composition, the PL intensity of a microrod incubated in the MABr solution was increased as shown in Figure 1e. Subsequently, the crystal was incubated in the MAI solution for 20-min. Like the microrod in Figure 1b, the initial $MAPbBr_3$ crystal was green emissive in the entire region [Figure 1f (i)]. Different from the case of an as-grown crystal without MABr treatment, the crystal pre-treated with MABr retained its green emission in the MAI solution [Figure 1f (ii)] even after a prolonged incubation. The initial PL spectral maximum was observed at 545 nm that was kept intact after the incubation in the MAI solution (Figure 1g). The low PL intensity of the MAI treated crystal is attributed to the following band distributions. The reduction in the PL intensity to one fourth of its initial value (Figure 1g) indicates the formation of low iodide composed $MAPb(Br{\cdot}I)_3$ from the $MAPbBr_3$ crystal. The energy gap between the conduction bands of $MAPbBr_3$ and $MAPbI_3$ is about 0.1 eV.[8] In the case of $MAPbBr_{3-n}I_n$ (n = 0 to 1), this

energy gap is comparable to the thermal energy at room temperature, allowing for the migration and localization of photogenerated electrons between $MAPbBr_3$ and $MAPbBr_{3-n}I_n$. Conversely, holes are trapped in the iodide rich region because of the higher valance band levels in $MAPb(Br.I)_3$, suppressing the radiative recombination after the exchange. To understand the role of such conduction and valance band states in $MAPbBr_3$ and $MAPb(Br.I)_3$ in the nonradiative recombination, and the PL intensity of a halide exchanged crystal, we measured the PL decays of the crystal before and after immersing in a MAI solution. We found a decrease (from 7 ns to 1 ns) in the PL lifetime of the crystal after immersing in a MAI solution (Figure S1]. As the result, the emission from the mixed halide crystal is quenched. Furthermore, the charge carrier segregation and nonradiative recombination quench the green PL (Figure 1f (ii) and g). In addition to the poor overlap between the electron and hole states, PL quenching and perovskite decomposition may occur through the vacancy-assisted oxidation of iodide ions.

The above PL image and spectral changes clearly indicate that the spontaneous halide exchange reaction of $MAPbBr_3$ with MAI is inhibited by treating the crystal with a MABr solution. The role of MABr to suppress the Br-to-I exchange reaction was examined using the plate-shaped $MAPbBr_3$ microcrystal [Figure S2]. The PL spectral data allow us to consider that the exchange reaction is inhibited by filling of the bromide vacancies using a MABr solution. It is proposed that the exchange reaction occurs *via* a vacancy-assisted diffusion mechanism.[9] Halide vacancies promote an efficient migration of halide ions inside a perovskite crystal, which results in the propagation of the exchange reaction from the surface to the bulk of a crystal.

To verify the role of laser irradiation on the filling of halide vacancies at the desired location, we selected $MAPbBr_3$ microrods and locally irradiated them with a 1064-nm focused laser beam (Figure 2a). Filling of halide vacancies in a $MAPbBr_3$ crystal with bromide ions is like its exchange reaction with iodide ions in view of the uptake of halide ions into the crystal. After preparing $MAPbBr_3$ microrods in a chamber, a reaction solution of MABr (250 μM) was added to the chamber [Figure 2a (i)]. Subsequently, the center area of the microrod was irradiated by a tightly focused NIR laser beam [Figure 2a (ii)]. After 20-min irradiation, the laser was switched off, the MABr solution was removed, and the chamber was incubated with the MAI (375 μM) reaction solution to examine if any bromide to iodide exchange reaction takes place [Figure 2a (iii)]. Figure 2b shows PL images of an as-grown $MAPbBr_3$ microrod crystal and the crystal in the reaction solution of MAI. The initial $MAPbBr_3$ crystal showed green emission in the whole area [Figure 2b (i)]. After the incubation in the MAI solution, the PL colour of the crystal at the non-irradiated area was gradually changed from green to red, where the vacancies were partially filled. Importantly, the irradiated central area remained green emissive [Figure 2b (ii)], where the halide exchange was locally suppressed by NIR laser-assisted filling of the Br vacancies. PL spectra of the crystal were measured in the MAI solution both

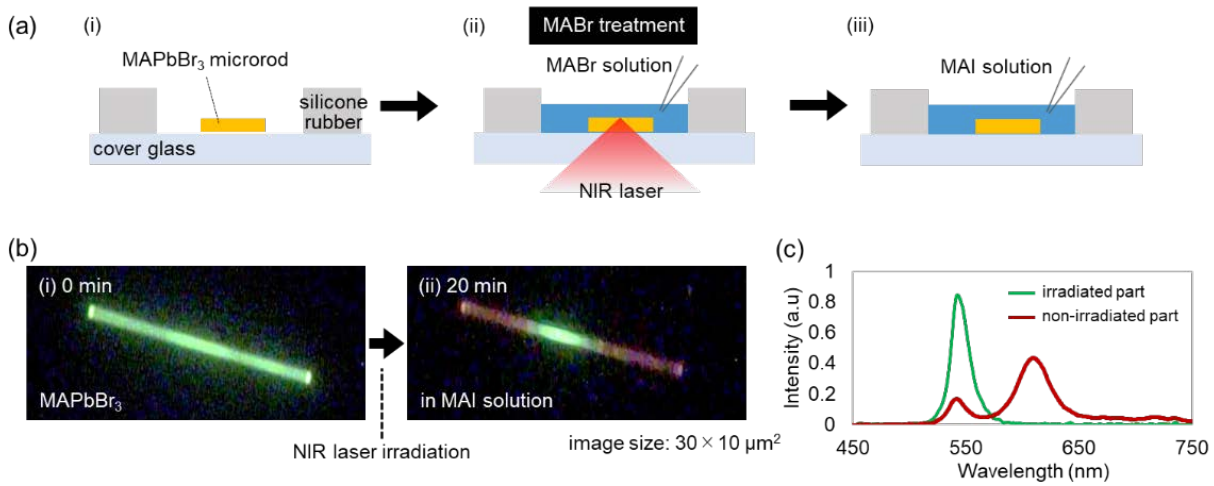

Figure 2. (a) A scheme of the experimental procedure for the laser irradiation to a $MAPbBr_3$ microrod in the solution. (b) PL images of (i) an as-grown $MAPbBr_3$ microrod crystal, and (ii) the crystal incubated in the MABr solution and irradiated at the center with the NIR laser and subsequently incubated in a MAI solution. (c) PL spectra of the crystal in a MAI reaction solution at the irradiated and non-irradiated areas.

from the non-irradiated and irradiated areas (Figure 2c). In the former area of the crystal, two PL peaks were observed at 545 nm and 615 nm, which are ascribed to the as-grown $MAPbBr_3$ and the halide exchanged $MAPb(Br{\cdot}I)_3$, respectively. Conversely, the irradiated centre part showed only one PL wavelength maximum (545 nm) similarly to the PL of the as-grown crystal. Thus, the irradiation by a focused laser beam locally fills the bromide vacancies in a $MAPbBr_3$ crystal immersed in a MABr reaction solution and inhibits the bromide to iodide exchange reaction when incubated in a MAI solution.

To understand the underlying mechanism of the spatially controlled inhibition of the exchange reaction, two-photon excited PL spectra from the centre of the crystal were recorded at equal time intervals while exciting with the focused NIR laser. There was no distinguishable change to the PL maximum of the irradiated area of the crystal immersed in a pure solvent [1-hexadecene/isopropanol (100:1)] (Figure 3a). Conversely, the PL intensity is increased more than 4 times in a MABr solution and saturated at 24 min (Figure 3b). After the irradiation into the central area of the crystal for 24 min, a PL spectrum was measured at the edge of the crystal by two-photon excitation with the NIR laser. The PL spectrum at the edge was essentially the same as the initial one (Figure 3b), and the PL intensity enhancement was observed only at the central irradiated area (Figure 3c).

To validate the relationship between localized vacancy filling and nonradiative carrier recombination, the PL lifetimes of the microrods were studied in the laser irradiated and non-irradiated areas. Along with a PL intensity enhancement, the PL lifetime of the microrod was different at the laser irradiated and non-irradiated areas (Figure 3d). The average PL lifetime at the non-irradiated area was 15 ns. Interestingly,

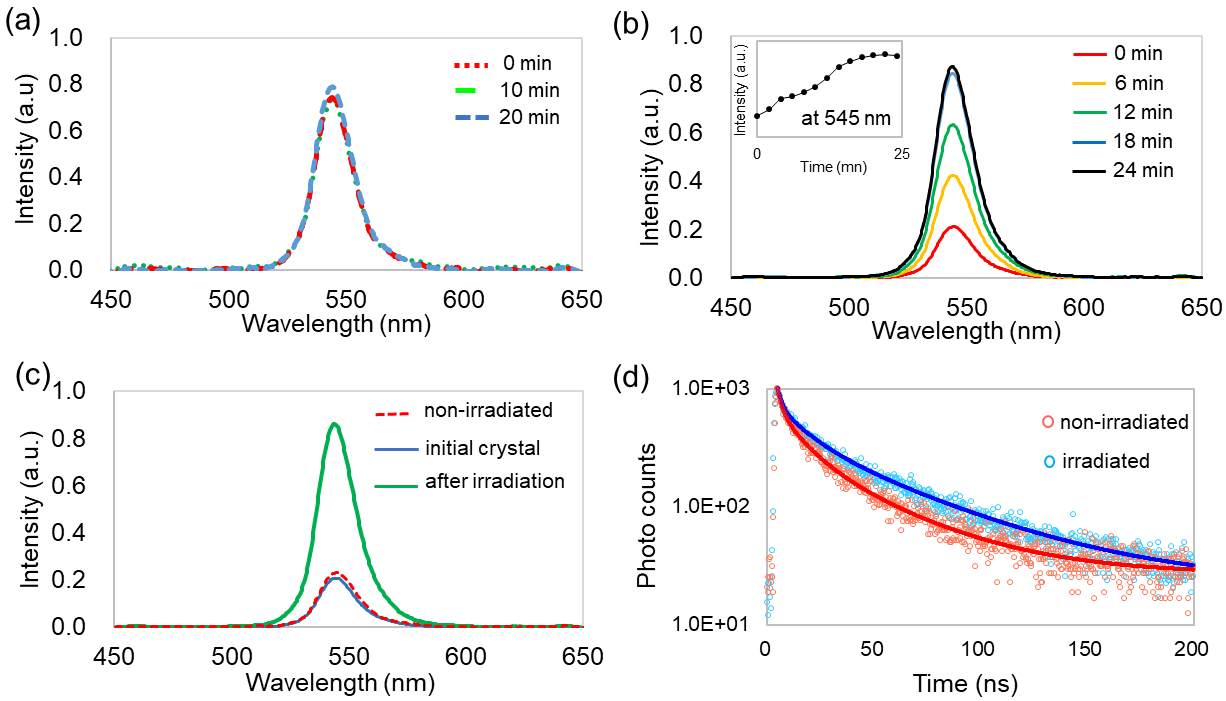

Figure 3. (a,b) Two-photon excited PL spectra of $MAPbBr_3$ microrods obtained in (a) a pure solvent without MABr and (b) in a MABr solution. Inset: the time evolution of the PL intensity at 545 nm. (c) PL spectra of an as-grown $MAPbBr_3$ microrod in a MAI reaction solution and measured at the laser irradiated and non-irradiated areas of the rod. (d) PL decay curves of the microrod at the laser irradiated and non-irradiated areas.

the PL lifetime was increased up to 23 ns by the NIR laser irradiation. Such an increase in lifetime was observed for all the microrods measured. The PL lifetime values at the non-irradiated parts were different among rods, which is due to a difference in the quality of the rods. Regardless of the initial PL lifetime, the laser irradiated area of a microrod consistently showed longer lifetime than a non-irradiated area. Thus, the NIR laser irradiation into a $MAPbBr_3$ crystal immersed in a MABr solution increased the PL intensity and lifetime. These changes suggest that the NIR laser irradiation decreases the density of halide vacancies at the irradiated area, which results in the suppression of nonradiative charge carrier recombination.

Here, we summarize the dynamics of inhibition of halide exchange reaction in $MAPbBr_3$ microrods. An as-grown $MAPbBr_3$ microrod contains many halide vacancies that traps photogenerated electrons. Bromide ions migrate inside a crystal *via* the halide vacancies. The exchange reaction with iodide ions proceeds through such an anion diffusion (Figure 4a)[10]. Upon the treatment of a $MAPbBr_3$ microrod with MABr, bromide ions fill the halide vacancies and improve the crystal quality. Thus, the PL intensity is increased and the PL lifetime becomes long. Also, anion migration inside the crystal is suppressed by filling the vacancies, and as the result, the exchange reaction is inhibited in the crystal pre-treated with MABr (Figure 4b). Such a filling of the halide vacancies is induced at the specific site of a $MAPbBr_3$ microrod immersed in a MABr reaction solution

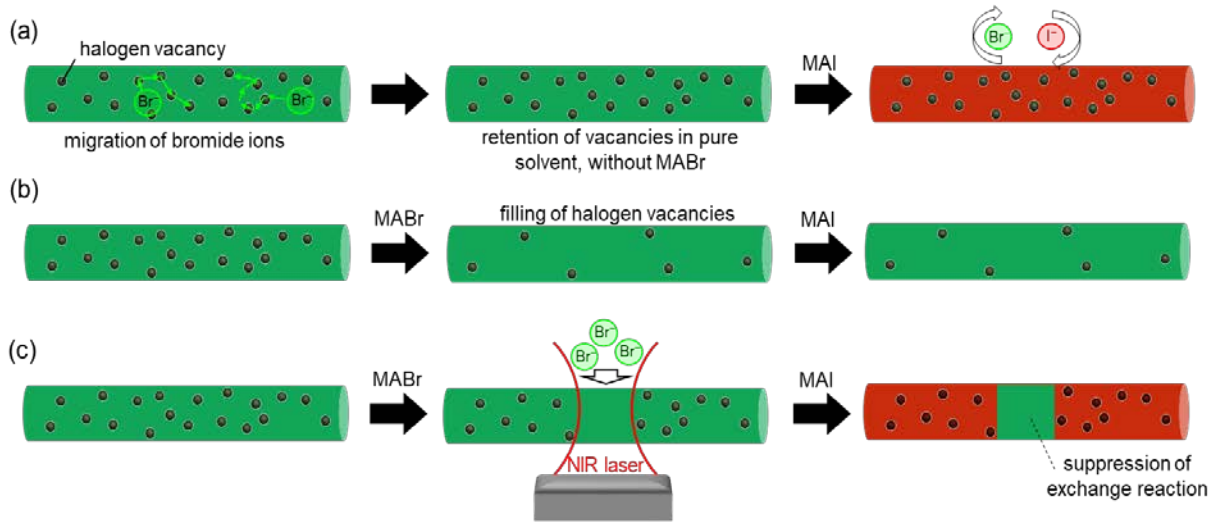

Figure 4. A scheme of halide vacancy filling and halide exchange suppression in $MAPbBr_3$ microrods. (a) The as-grown microrod immersed in a solvent, but without any MABr and then treated with MAI. (b) A microrod immersed in a MABr solution and then in a MAI solution. (c) A microrod immersed in a low concentration solution of MABr, irradiated at the center with the 1064 nm focused laser beam, and then immersed in a MAI solution.

by irradiating the focused NIR laser beam. The Br-to-I exchange reaction in a $MAPbBr_3$ microrod takes place exclusively in the non-irradiated areas (Figure 4c). Conversely, Br vacancies were filled in the irradiated area.

We consider that Br^- vacancies in the irradiated part of a microrod is efficiently filled by NIR laser irradiation.[11] Since the pioneer report by Ashkin *et.al* in 1986 on optical trapping of particles using a single beam gradient force,[12] optical force is often being utilized for patterning of nanoparticles,[13] crystallization of molecular and ionic compounds,[14] and controlling phase transition or separation spatiotemporally.[15] The applied optical force on a nm-size object using a focused laser beam is proportional to the volume of the target object. However, the reactive halide precursors are too small to realize the laser trapping force. Thus, we propose the following mechanisms to account for the localized halide exchange and rule out the effect of temperature and light. We consider that due to the strong optical force generated by the focused laser beam, a group of the precursors comes to the focal spot and remains there. Also, the diffusion of such a group of molecules is two-dimensionally suppressed at the solid/liquid interface. Although the dynamics of laser trapping is unsolved at the present stage, we infer that an increase in the concentration of MABr contributes to local filling of the Br vacancies.

In summary, we have successfully shown a facile post-synthesis method to control the anion exchange reactions of halide perovskite microrod single crystals. The exchange reaction is inhibited by treating the crystal with the constituent halide ions to fill the vacancies. We have also demonstrated the inhibition of such anion exchange reaction in a site-selective manner by irradiating a focused NIR laser. Thus, these findings offer a new methodology for spatially resolved halide vacancy filling and improving the

properties of perovskite materials toward the fabrication of high-quality semiconductor heterojunction devices.

References

[1] a) M. L. Petrus, T. Bein, T. J. Dingemans, P. Docampo, *J. Mater. Chem. A* **2015**, *3*, 12159–12162; b) A. Sadhanala, S. Ahmad, B. Zhao, N. Giesbrecht, P. M. Pearce, F. Deschler, R. L. Z. Hoye, K. C. Gödel, T. Bein, P. Docampo, S. E. Dutton, M. F. L. De Volder, R. H. Friend, Nano Lett. 2015, 15, 6095–6101; c) N. J. Jeon, J. H. Noh, W. S. Yang, Y. C. Kim, S. Ryu, J. Seo, S. Il Seok, *Nature* **2015**, *517*, 476–480; d) J. H. Heo, M. H. Lee, H. J. Han, B. R. Patil, J. S. Yu, S. H. Im, *J. Mater. Chem. A* **2016**, *4*, 1572–1578; e) Z. K. Tan, R. S. Moghaddam, M. L. Lai, P. Docampo, R. Higler, F. Deschler, M. Price, A. Sadhanala, L. M. Pazos, D. Credgington, F. Hanusch, T. Bein, H. J. Snaith, R. H. Friend, *Nat. Nanotechnol.* **2014**, *9*, 687–692; f)Y. Fu, H. Zhu, C. C. Stoumpos, Q. Ding, J. Wang, M. G. Kanatzidis, X. Zhu, S. Jin, *ACS Nano* **2016**, *10*, 7963–7972.

[2] a) C. Eames, J. M. Frost, P. R. F. Barnes, B. C. O'Regan, A. Walsh, M. S. Islam, *Nat. Commun.* **2015**, *6*, 2–9; b) V. D'Innocenzo, G. Grancini, M. J. P. Alcocer, A. R. S. Kandada, S. D. Stranks, M. M. Lee, G. Lanzani, H. J. Snaith, A. Petrozza, *Nat. Commun.* **2014**, *5*, 1–6; c) C. Wehrenfennig, G. E. Eperon, M. B. Johnston, H. J. Snaith, L. M. Herz, *Adv. Mater.* **2014**, *26*, 1584–1589; d) F. Liu, Y. Zhang, C. Ding, S. Kobayashi, T. Izuishi, N. Nakazawa, T. Toyoda, T. Ohta, S. Hayase, T. Minemoto, K. Yoshino, S. Dai, Q. Shen, *ACS Nano* **2017**, *11*, 10373–10383.

[3] a) D. M. Jang, K. Park, D. H. Kim, J. Park, F. Shojaei, H. S. Kang, J. P. Ahn, J. W. Lee, J. K. Song, *Nano Lett.* **2015**, *15*, 5191–5199; b) D. Parobek, Y. Dong, T. Qiao, D. Rossi, D. H. Son, *J. Am. Chem. Soc.* **2017**, *139*, 4358–4361; c) I. Karimata, Y. Kobori, T. Tachikawa, *J. Phys. Chem. Lett.* **2017**, *8*, 1724–1728; d) D. Zhang, Y. Yang, Y. Bekenstein, Y. Yu, N. A. Gibson, A. B. Wong, S. W. Eaton, N. Kornienko, Q. Kong, M. Lai, A. P. Alivisatos, S. R. Leone, P. Yang, *J. Am. Chem. Soc.* **2016**, *138*, 7236–7239.

[4] a) G. Landi, H. C. Neitzert, C. Barone, C. Mauro, F. Lang, S. Albrecht, B. Rech, S. Pagano, *Adv. Sci.* **2017**, *4*, 1700183-93; b) P. Xu, S. Chen, H. J. Xiang, X. G. Gong, S. H. Wei, *Chem. Mater.* **2014**, *26*, 6068–6072.

[5] a) S. Cacovich, F. Matteocci, M. Abdi-Jalebi, S. D. Stranks, A. D. Carlo, C. Ducati, G. Divitini, *ACS Appl. Energy Mater.* **2018**, *1*, 7174−7181; b) W. Wu, P. N. Rudd, Z. Ni, C. H. V. Brackle, H. Wei, Q. Wang, B. R. Ecker, Y. Gao, J.Huang, *J. Am. Chem. Soc.* **2020**, *142*, 3989−3996.

[6] M. I. Saidaminov, A. L. Abdelhady, G. Maculan, O. M. Bakr, *Chem. Commun.* **2015**, *51*, 17658–17661.

[7] K. H. Wang, L. C. Li, M. Shellaiah, K. W. Sun, *Sci. Rep.* **2017**, *7*, 1–14.

[8] P. Schulz, E. Edri, S. Kirmayer, G. Hodes, A. Kahn, *Energy Environ. Sci.* **2014**, *7*, 1377–1381.

[9] a) J. Mizusaki, K. Arai, K. Fueki, *Solid State Ionics* **1983**, *11*, 203–211; b) M. Lai, A. Obliger, D. Lu, C. S. Kley, C. G. Bischak, Q. Kong, T. Lei, L. Dou, N. S. Ginsberg, D. T. Limmer, P. Yang, *Proc. Natl. Acad. Sci. U. S. A.* **2018**, *115*, 11929–11934.

[10] M. Laia, A. Obligera, D.Lua, C. S. Kleya, C. G. Bischaka, Q. Konga, T. Leia, L. Doua, N. S.Ginsberga, D. T. Limmera, P. Yang, *PNAS* **2018**, *115*, 11929–11934.

[11] M. J. Islam, M. Shahjahan, K. I. Yuyama, V. Biju, *ACS Mater. Lett.* **2020**, *2*, 403–408.

[12] A. Ashkin, J. M. Dziedzic, J. E. Bjorkholm, S. Chu, *Opt. Lett.* **1986**, *11*, 288–290.

[13] a) S. Ito, H. Yoshikawa, H. Masuhara, *Appl. Phys. Lett.* **2001**, *78*, 2566–2568; b) M. J. Guffey, N. F. Scherer, *Nano Lett.* **2010**, *10*, 43024308.

[14] a) J. Hofkens, J. Hotta, K. Sasaki, H. Masuhara, K. Iwai, *Langmuir* **1997**, *13*, 414–419; b) W. Singer, T. A. Nieminen, N. R. Heckenberg, H. Rubinsztein-Dunlop, *Phys. Rev. E* **2007**, *75*, 1–5; c) Y. Tsuboi, T. Shoji, N. Kitamura, *J. Phys. Chem. C* **2010**, *114*, 5589–5593; d) T. Shoji, N. Kitamura, Y. Tsuboi, *J. Phys. Chem. C* **2013**, *117*, 10691–10697.

[15] a) S. A. Mukai, N. Magome, H. Kitahata, K. Yoshikawa, *Appl. Phys. Lett.* **2003**, *83*, 2557–2559; b) T. Sugiyama, T. Adachi, H. Masuhara, *Chem. Lett.* **2007**, *36*, 1480–1481; c) K. I. Yuyama, M. J. Islam, K. Takahashi, T. Nakamura, V. Biju, *Angew. Chemie - Int. Ed.* **2018**, *57*, 13424–13428.